

Single cell mechanics: stress stiffening and kinematic hardening

Pablo Fernández* and Albrecht Ott†

Experimentalphysik I, Physikalisches Institut, Universität Bayreuth, D-95440 Bayreuth, Germany

(Dated: October 22, 2018)

Cell mechanical properties are fundamental to the organism but remain poorly understood. We report a comprehensive phenomenological framework for the nonlinear rheology of single fibroblast cells: a superposition of elastic stiffening and viscoplastic kinematic hardening. Our results show, that in spite of cell complexity its mechanical properties can be cast into simple, well-defined rules, which provide mechanical cell strength and robustness via control of crosslink slippage.

PACS numbers: 87.15.La, 83.60.Df, 83.60.La, 87.16.Ka

Intracellular transport, cell locomotion, resistance to external mechanical stress and other vital biomechanical functions of eukaryotic cells are governed by the cytoskeleton, an active biopolymer gel [1]. This gel is made of three types of biopolymers, actin, microtubules and intermediate filaments, crosslinked by a multitude of proteins with different properties in terms of connection angles, bond strengths and bond lifetimes. The actin cytoskeleton –the major force-sustaining structure in our experiments– is made of filaments of about micrometer length and presents a weak local structural order. The cytoskeleton also comprises molecular motors, proteins that move on actin or microtubule filaments driven by chemical energy. How the cytoskeleton in conjunction with biochemical regulatory circuits performs specific, active mechanical tasks is not understood. When cells attach to biological material they often biochemically recognize the binding partner. The cytoskeleton organizes accordingly and produces a mechanical response. Active cell responses such as contraction are well separated from passive rheological properties by their timescales [2]. Passive rheological cell properties have been studied with various techniques on subcellular and supercellular scale [3]. From the measurements with different techniques on different eukaryotic cell types a broad relaxation spectrum arises as a common feature of passive, linear cell rheology [3, 4]. The description of the non-linear regime remains elusive; both stiffening [5, 6, 7, 8, 9] and linear responses to large stretch [8, 9, 10, 11] have been observed.

In the following we present microplate rheology experiments where individual cells are stretched between two plates (Fig. 1). The advantage of the setup is that the cells possess a well-controlled geometry and adhere via chosen biochemical linkers, which better define the cytoskeletal state. Quasi-differential cell deformations reveal an elastic stiffening response. The corresponding nonlinear elastic modulus depends on the cell prestress

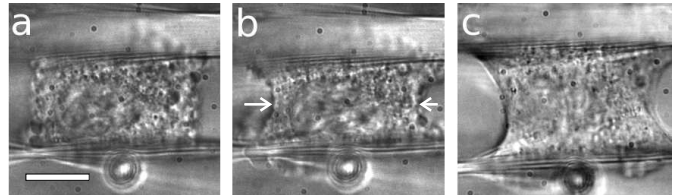


Figure 1: A fibroblast adhering between two microplates. **a:** Right after contact. Bar: 10 μm . **b:** After ~ 20 min at 35°C , strongly adhering cells often adopt a concave shape. From the apparent diameter D_0 (arrows) we estimate the initial area $A_0 := \pi(D_0/2)^2$. **c:** Under large stretch.

but is independent of cell length. Large deformations reveal an inelastic regime with a (counterintuitive) linear force-length relation. Both relations simply superpose to generate the response to more complex deformations. The cell response reduces to the integral of the differential measurement when the inelastic response is abolished by fixation. Hence, in spite of the complexity of the eukaryotic cell cytoskeleton and large cell heterogeneity, passive nonlinear cell rheology can be reduced to simple rules.

Experimental setup.— We refer to [2, 7, 12] for details. A 3T3 fibroblast [13] adheres between two fibronectin-coated glass microplates. One of them is flexible: its deflection gives the perpendicular force F acting on the cell. This plate is translated by a piezoelectric actuator controlled by a personal computer. The computer calculates force F and cell length ℓ , and adjusts the piezo position via a proportional feedback loop to impose a given experimental protocol. Experiments are performed at 35°C , in standard medium with Lysophosphatidic acid 50 μM (Sigma). Cells are left to adhere for 30 min before measuring. All results described here are fully reproducible for fibroblasts which adhere sufficiently strongly to sustain pulling forces of 100 nN for several hours, which means about 30% of the cells in culture.

Loading and unloading at constant rate— We stretch the cell by 100% at a constant rate $\dot{\ell}$ while measuring the force F (Fig. 2a). The slope $dF/d\ell$ initially decreases, reaching a constant value at an elongation $\sim 10\%$ (Fig. 2b). Beyond 10% and up to 100% stretch, the $F(\ell)$ relation is in most cases linear. After loading, the cell

*Present address: Lehrstuhl für Biophysik E22, Technische Universität München, James Franck Straße, D-85748 Garching, Germany

†Present address: Biologische Experimentalphysik, Universität des Saarlandes, D-66041 Saarbrücken, Germany

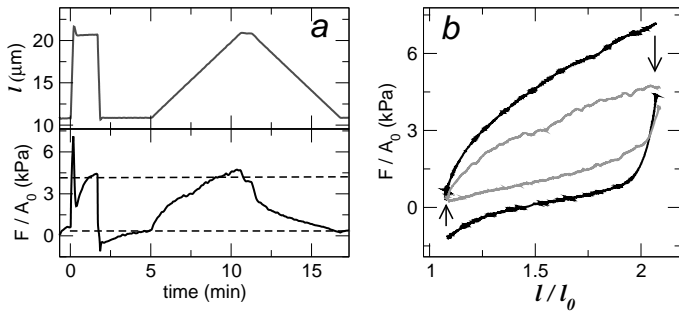


Figure 2: Loading and unloading at constant rate \dot{l} . **a**: length l and lagrangian stress F/A_0 (where A_0 is the initial area) as a function of time. After each ramp, F stabilizes at a nonzero value \mathfrak{F} (dotted line). **b**: F/A_0 as a function of l/l_0 (where l_0 is the steady zero-force length) during loading and unloading. Black curve: $\dot{l} = 1 \mu\text{m/s}$. Grey curve: $\dot{l} = 0.03 \mu\text{m/s}$.

length l is held constant for a few minutes; the force F relaxes to a steady non-zero value \mathfrak{F} which does not evolve faster than $\sim 1 \text{ nN/s}$. An analogous response is observed upon unloading. The procedure is repeated with different rates \dot{l} between 3 nm/s and $10 \mu\text{m/s}$. The asymptotic slope dF/dl and the equilibrium force \mathfrak{F} are independent of the loading rate in the explored range.

Small amplitude stiffening, large amplitude linearity— To explore small and large deformation amplitudes simultaneously we perform a loading ramp with superimposed harmonic oscillations, imposing $l(t) = vt + \Delta_\ell \sin(\omega t)$. Fig. 3 shows a typical experiment. The response to small oscillations indeed stiffens with increasing stress. Yet, the averages over an oscillation period of the force $\langle F \rangle$ and length $\langle \ell \rangle$ are linearly related as inferred from the position of the loops. Therefore, we observe both responses *simultaneously*: stiffening at small amplitudes, as

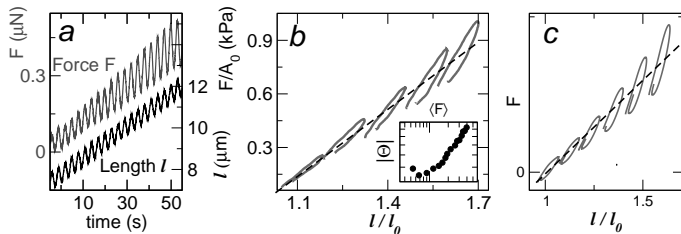


Figure 3: Small amplitude stiffening, large amplitude linearity. **a**: F and l as a function of time. **b**: F/A_0 as a function of l/l_0 . For clarity, only a few loops are shown. The dashed line highlights the linear relation between the average values. **Inset**: Differential modulus $|\Theta|$ as a function of average force $\langle F \rangle$ for the data shown in b. The response to the small oscillations shows stiffening, following the master-relation reported in [7]. **c**: Eqs. 1–4 taking $\gamma = 5$ and $\mathcal{D} = 0.01 \partial F/\partial \lambda$.

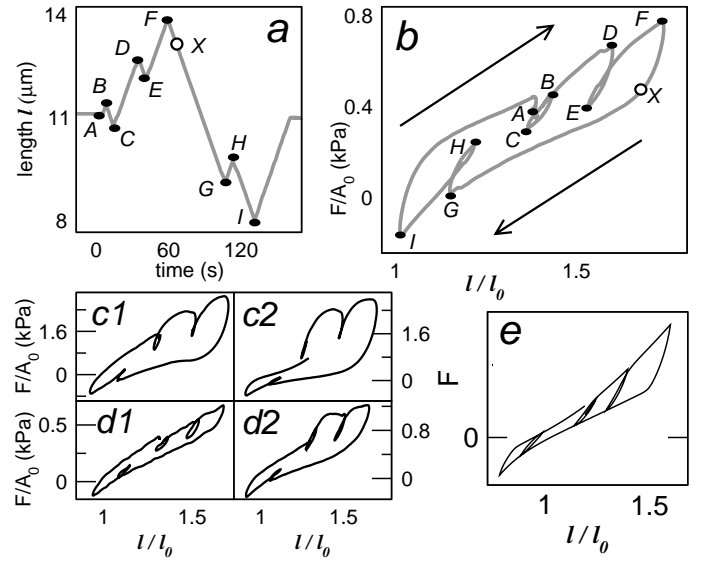


Figure 4: Elastic / inelastic behavior. **a**: Imposed length l as a function of time. **b**: F/A_0 as a function of l/l_0 for a given cell. Reversible (elastic) behavior upon direction reversal is observed only close to a previous turning point, as in C, E, H. The response becomes irreversible (inelastic) after a steady large deformation: at the turning points D, F, G, I, the $F(l)$ curve does not retrace its previous path. Between F and I the experiment is equivalent to C–F, but in the unloading direction. The response is seen to be equivalent, showing the sense of deformation to be irrelevant. **c1**: Another cell, probed at a rate $\dot{l} = 0.1 \mu\text{m/s}$. **c2**: Same cell as c1 but at $\dot{l} = 1 \mu\text{m/s}$. **d1**: Another cell, $0.1 \mu\text{m/s}$. **d2**: Same cell as d1, $1 \mu\text{m/s}$. **e**: Prediction of the constitutive relation (Eqs. 1–4).

reported in [7], and linearity at large amplitudes.

Small amplitude reversibility, large amplitude irreversibility— We study the amplitude dependence at a constant deformation rate $|\dot{l}|$. An essential feature of the protocol (Fig. 4a) are the turning points separated at various distances in order to study the reversibility of the response. Similar procedures can be found in plasticity textbooks [14]. As Fig. 4b shows, the reversibility of the response upon a change of direction is determined *by the distance to the previous turning point*. Where turning points are separated by less than 10% stretch, the response is reversible (elastic). More than 10% stretch beyond a turning point, the response becomes irreversible (inelastic): the $F(l)$ curve does not retrace its path upon direction reversal. In this inelastic regime the $F(l)$ relation is approximately linear. Its nonzero slope leads to *a translation of the elastic region by the inelastic deformation*, a behavior known in plasticity as linear kinematic (or directional) hardening [14, 15, 16, 17]. Alternatively, the inelastic *contraction* under *pulling* tension between X and G in Fig. 4b is a strong Bauschinger effect (a decrease in yield stress upon unloading) [14, 18].

Large amplitude stiffening after glutaraldehyde

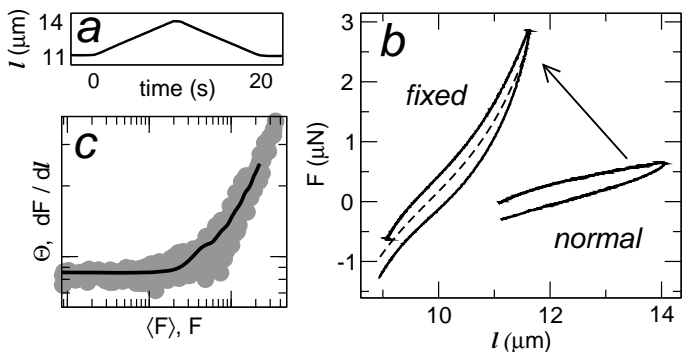


Figure 5: **a**: Imposed length ℓ as a function of time. A single loading cycle with amplitude 30% is performed. **b**: Force F as a function of length ℓ . “Normal”: before adding glutaraldehyde. “Fixed”: in presence of glutaraldehyde 0.1%. The dotted line is a fit to Eq.2. **c**: The derivative $dF/d\ell$ of the “fixed” curve (black line) plotted against the differential master-relation (gray dots, as discussed in Ref.[7]).

fixation.— We add glutaraldehyde 0.1% in order to prevent slippage of cytoskeletal connections. Loading at constant rate (Fig. 5a) reveals a *positive curvature* $d^2F/d\ell^2$ (Fig. 5b). The numerical derivative of the $F(\ell)$ relation obtained from fixed (hence dead) cells is the same as the differential master-relation obtained on *living* fibroblasts (Fig. 5c, from Ref. [7]). The $F(\ell)$ relation after fixation closely resembles the exponential stress-stretch relations known from whole tissues [19, 20].

Rate dependence.— In the inelastic regime the width of the hysteresis loops increases with stretch rate (Fig. 6a). To characterize this rate-dependence, we define the overstress ΔF as the extent of force relaxation after unloading (Fig. 6a). The overstress ΔF behaves as $\log(d\ell/dt)$, approaching zero at a non-zero pulling speed of about 10 nm/s (Fig.6b). Below such rates the behavior becomes active and erratic and the overstress ill-defined.

Viscoplasticity.— We now propose a minimal constitutive relation for fibroblasts under uniaxial extension. First we decompose the measurable cell length ℓ into inelastic rest length \mathfrak{L} and elastic stretch ratio λ ,

$$\ell = \lambda \mathfrak{L}. \quad (1)$$

The force is a function solely of the elastic strain,

$$F \propto (\lambda - 1)e^{\gamma(\lambda^2 + 2/\lambda - 3)}, \quad (2)$$

where for concreteness we use exponential elasticity [19], according to Fig. 5b, c. As a flow rule relating the inelastic strain rate $\dot{\mathfrak{L}}$ to the force F , we propose an exponential function of the overstress $F - \mathfrak{F}$, according to Fig. 6b:

$$\dot{\mathfrak{L}} = v \operatorname{sgn}(F - \mathfrak{F}) e^{|F - \mathfrak{F}|/D}, \quad (3)$$

with a vanishing dissipation as the flow rate $\dot{\mathfrak{L}}$ approaches v . The equilibrium force \mathfrak{F} is the essential internal variable to describe kinematic hardening [14, 15, 17]. The

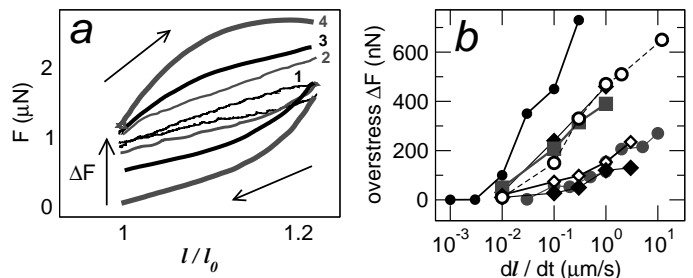


Figure 6: Loading and unloading for several rates $\dot{\ell}$. **a**: F as a function of ℓ/ℓ_0 for a given cell, where ℓ_0 is the initial length. Rates are: 1) 10 nm/s, 2) 30 nm/s, 3) 0.1 $\mu\text{m/s}$, 4) 1 $\mu\text{m/s}$. The overstress ΔF is defined as the extent of relaxation after unloading. **b**: ΔF as a function of rate $\dot{\ell}$ for 7 different cells.

drag force \mathcal{D} sets the scale where the overstress induces inelastic flow. To obtain an increased dissipation at large forces (e.g. the increase in the area of the loops in Fig. 3), we take the drag \mathcal{D} as proportional to the nonlinear modulus, $\partial F/\partial \lambda$. Finally, we have linear kinematic hardening:

$$\mathfrak{F} \propto \dot{\mathfrak{L}}. \quad (4)$$

This is an empiric description along the lines of modern viscoplasticity [14, 17, 18], without explicit history dependencies. As Figs. 3c and 4e show, it captures the essence of the phenomenology. At small amplitudes, $|F - \mathfrak{F}| \ll \mathcal{D}$, the deformation is essentially elastic: $\dot{\ell} \sim \dot{\lambda}$. At large amplitudes the overstress $|F - \mathfrak{F}|$ approaches the drag stress \mathcal{D} and the deformation becomes increasingly inelastic: $\dot{\ell} \sim \dot{\mathfrak{L}} \propto \mathfrak{F} \sim \dot{F}$. Nevertheless, this constitutive relation is not yet a full description. The details of the linear regime [4, 11] and fluidization at large flow rates [7] still have to be incorporated to it, whereas active contraction and inelastic deformation at rates below v , as well as the force fluctuations seen in Fig. 2 may require a different approach.

Discussion.— Our glutaraldehyde fixation experiments show that stress stiffening in fibroblasts [7] is due to the nonlinear elasticity of the cytoskeleton, unrelated to biological signalling or restructuring. In agreement, very similar stiffening is known from biopolymer networks [21]. To date the precise microscopic mechanism remains unclear; stretching [21, 22] and bending [7, 23] of single filaments as well as filament alignment [24] have been proposed.

The energy to reach the linear inelastic regime in loading experiments (from Fig. 2) is $\sim 1\mu\text{N}\mu\text{m} \simeq 2.5 \cdot 10^8 k_B T$. During stretch, first elastic elements must be loaded, until they dissipate the stored energy upon bond rupture. Taking typical orders of magnitude for bond energies [25] and dissipation [26] and a mesh size of 100 nm [1], over 10% of the actin cytoskeletal bonds must be ruptured to reach stationary flow. However, in order to observe stress stiffening ubiquitously during the inelastic deformation, the actin gel must be always above

percolation threshold. For a gel with one bond relaxation time one expects a rate-independent overstress [27]; we observe an exponential rate-overstress dependence. In general, dissociation rates depend on the force per bond f as $\sim e^{f/f_0}$, with a force scale $f_0 \sim 10$ pN [28, 29]. In agreement, in fibroblasts the drag \mathcal{D} is about 100 nN, corresponding to 1–10 pN per filament. Interestingly, the inelastic stretch rate where the cell flows without hysteresis is of the order of 10^{-3}s^{-1} , a typical rate for active processes such as crawling and contraction [1, 3]. Thus, spontaneous bond dissociation may be what limits active phenomena to long timescales [2].

A living cell can neither be purely elastic, nor possess a yield stress within the physiological “working range”. Kinematic hardening viscoplasticity can be understood as a consequence of these conditions. Combined with a sharply rising rate-overstress dependence, it prevents cell breakage in our large deformation experiments: a cell portion under increased stress will readily flow and increase its equilibrium stress to reach a stable situation. Rather than break at a given spot, the cell prolongs homogeneously along its length. This homogeneous deformation may be behind the robust linearity of the kinematic hardening response, since integration of a constant magnitude along the cell length naturally gives a linear length-dependence. However, identification of the precise molecular mechanisms behind this unusual behavior in a

soft system is a task for the future. At least, one can rule out a trivial interpretation in terms of a Hookean spring element (in form of intermediate filaments, for example) in parallel with a stiffening viscoelastic liquid: since the liquid cannot sustain an average stress, a non-mechanical coupling between the two elements is needed for the cell to stress-stiffen. Thus, in a mechanical interpretation hardening and stiffening must originate in one and the same mechanical element. If intermediate filaments [1] play a role, they must be interconnected with actin into a single network. This scenario reminds of composite alloys [18] and granular materials [16], where kinematic hardening arises as the inelastic flow induces alterations of directional nature to the microstructure.

Summarizing, we have shown that cell mechanical properties in uniaxial stretching experiments can be thoroughly described by the superposition of two simple relations: exponential elasticity, and viscoplasticity with linear kinematic hardening. Given the cytoskeletal complexity, this is unexpected. A complete picture of passive cell rheology spanning from molecular details to a simple phenomenological description and straightforward theoretical concepts seems in close reach.

We thank P. A. Pullarkat for his invaluable advice, and K. Kroy for inspiring discussions and support. This work has been funded by the Universität Bayreuth.

-
- [1] D. Bray, *Cell Movements : from molecules to motility* (Garland Publishing, Inc., New York, 2001), 2nd ed.
- [2] O. Thoumine and A. Ott, *J. Cell. Sci.* **110**, 2109 (1997).
- [3] P. A. Pullarkat, P. A. Fernández, and A. Ott, *Phys. Rep.* **449**, 29 (2007).
- [4] B. Fabry, G. N. Maksym, J. P. Butler, M. Glogauer, D. Navajas, and J. J. Fredberg, *Phys. Rev. Lett.* **87**, 148102 (2001).
- [5] N. Wang, J. P. Butler, and D. E. Ingber, *Science* **260**, 1124 (1993).
- [6] N. Wang, I. M. Tolic-Nørrelykke, J. Chen, S. M. Mijailovich, J. P. Butler, J. J. Fredberg, and D. Stamenović, *Am. J. Physiol. Cell Physiol.* **282**, C606 (2002).
- [7] P. Fernández, P. A. Pullarkat, and A. Ott, *Biophys. J.* **90**, 3796 (2006).
- [8] T. Wakatsuki, M. S. Kolodney, G. I. Zahalak, and E. L. Elson, *Biophys. J.* **79**, 2353 (2000).
- [9] P. Fernández, L. Heymann, A. Ott, N. Aksel, and P. A. Pullarkat, *New J. Phys.* (2007).
- [10] S. Yang and T. Saif, *Exp. Cell Res.* **305**, 42 (2005).
- [11] N. Desprat, A. Richert, J. Simeon, and A. Asnacios, *Biophys. J.* **88**, 2224 (2005).
- [12] P. Fernández, Ph.D. thesis, Universität Bayreuth (2006).
- [13] G. J. Todaro and H. Green, *J. Cell. Biol.* **17**, 299 (1963).
- [14] J. Lubliner, *Plasticity theory* (Macmillan Publishing Company, New York, 1990), 1st ed.
- [15] W. Prager and H. Geiringer, *Ergebnisse der exakten Naturwissenschaften* **13** (1934).
- [16] S. Nemat-Nasser, *Plasticity: A Treatise on Finite Deformation of Heterogeneous Inelastic Materials* (Cambridge University Press, 2004).
- [17] E. Krempl, in *Unified constitutive laws of plastic deformation*, edited by A. S. Krausz and K. Krausz (Academic Press, San Diego, 1996), pp. 281–318.
- [18] U. F. Kocks, in *Unified constitutive equations for creep and plasticity*, edited by A. Miller (Elsevier applied sciences, Essex, 1987), pp. 1–88.
- [19] Y. C. Fung, *Biomechanics: Mechanical properties of living tissues* (Springer Verlag, New York, 1993).
- [20] Exponential elasticity can also be revealed by microrheological techniques. B. Fabry, personal communication.
- [21] C. Storm, J. J. Pastore, F. C. MacKintosh, T. C. Lubensky, and P. A. Janmey, *Nature* **435**, 191 (2005).
- [22] E. Kuhl, K. Garikipati, E. M. Arruda, and K. Grosh, *J. Mech. Phys. Solids* **53**, 1552 (2005).
- [23] A. Kabla and L. Mahadevan, *J. R. Soc. Interface* **4**, 99 (2007).
- [24] P. R. Onck, T. Koeman, T. van Dillen, and E. van der Giessen, *Phys. Rev. Lett.* **95**, 178102 (2005).
- [25] A. Mogilner and G. Oster, *Biophys. J.* **71**, 3030 (1996).
- [26] E. Décavé, D. Garrivier, Y. Bréchet, F. Bruckert, and B. Fourcade, *Phys. Rev. Lett.* **89**, 108101 (2002).
- [27] F. Gerbal, V. Noireaux, C. Sykes, F. Jülicher, P. Chaikin, A. Ott, J. Prost, R. M. Golsteyn, E. Friederich, D. Louvard, et al., *Pramana - J. Phys.* **53**, 155 (1999).
- [28] G. I. Bell, *Science* **200**, 618 (1978).
- [29] D. A. Simson, M. Strigl, M. Hohenadl, and R. Merkel, *Phys. Rev. Lett.* **83**, 652 (1999).